



Published in final edited form as:

J Am Coll Surg. 2012 July ; 215(1): 126–135. doi:10.1016/j.jamcollsurg.2012.02.021.

Fluorescence-Guided Surgery Allows for More Complete Resection of Pancreatic Cancer Resulting in Longer Disease-Free Survival Compared to Standard Surgery in Orthotopic Mouse Models

Cristina A Metildi, MD¹, Sharmeela Kaushal, PhD¹, Chanae Hardamon, BSc¹, Cynthia S Snyder, MD¹, Minya Pu, PhD¹, Karen S Messer, PhD¹, Mark A Talamini, MD, FACS¹, Robert M Hoffman, PhD^{1,2}, and Michael Bouvet, MD, FACS¹

¹Department of Surgery, University of California San Diego, San Diego, CA

²AntiCancer, Inc, San Diego, CA

Abstract

Background—Negative surgical margins are vital to achieve cure and prolong survival in patients with pancreatic cancer. We inquired if fluorescence-guided surgery (FGS) could improve surgical outcomes and reduce recurrence rates in orthotopic mouse models of human pancreatic cancer.

Study Design—A randomized active-control pre-clinical trial comparing bright light surgery (BLS) to fluorescence-guided surgery (FGS) was utilized. Orthotopic mouse models of human pancreatic cancer were established using the BxPC-3 pancreatic cancer cell line expressing red fluorescent protein (RFP). Two weeks after orthotopic implantation, tumors were resected with BLS or FGS. Pre- and postoperative images were obtained with the OV-100 Small Animal Imaging System to assess completeness of surgical resection. Postoperatively, whole body imaging was done to assess recurrence and follow tumor progression. Six weeks postoperatively, mice were sacrificed to evaluate primary pancreatic and metastatic tumor burden.

Results—A more complete resection of pancreatic cancer was achieved using FGS compared to BLS: 98.9% vs. 77.1%, $p=0.005$. The majority of mice undergoing BLS (63.2%) had evidence of gross disease with no complete resections, whereas 20% of mice undergoing FGS had complete resection and an additional 75% had only minimal residual disease ($p=0.0001$). The mean postoperative tumor burden was significantly less with FGS compared to BLS: $0.08 \pm 0.06 \text{ mm}^2$ vs. $2.64 \pm 0.63 \text{ mm}^2$, $p=0.001$. The primary tumor burden at termination was significantly less with FGS compared to BLS: $19.3 \pm 5.3 \text{ mm}^2$ vs. $6.2 \pm 3.6 \text{ mm}^2$, $p=0.048$. FGS resulted in significantly longer disease-free survival than BLS ($p=0.02$, HR=0.39, 95% CI: (0.17, 0.88)).

© 2012 American College of Surgeons. Published by Elsevier Inc. All rights reserved.

Correspondence address: Michael Bouvet, MD, Department of Surgery, Moores UCSD Cancer Center, 3855 Health Science Drive #0987, La Jolla, CA 92093-0987, Phone: 858-822-6191, Fax: 858-822-6192, mbouvet@ucsd.edu.

Presented at the Western Surgical Association 119th Scientific Session, Tucson, AZ, November 2011.

Disclosure Information: Dr Hoffman is a stockholder and is president of AntiCancer, Inc., but does not receive a salary. All other authors have nothing to disclose.

Publisher's Disclaimer: This is a PDF file of an unedited manuscript that has been accepted for publication. As a service to our customers we are providing this early version of the manuscript. The manuscript will undergo copyediting, typesetting, and review of the resulting proof before it is published in its final citable form. Please note that during the production process errors may be discovered which could affect the content, and all legal disclaimers that apply to the journal pertain.

Conclusions—Surgical outcomes were improved in pancreatic cancer using fluorescence-guidance. This novel approach has significant potential to improve surgical treatment of cancer.

Keywords

pancreatic cancer; orthotopic mouse models; surgery; fluorescence; resection; recurrence; survival

Introduction

Currently, surgical resection of pancreatic cancer remains the only curative option for this disease.¹ Surgical resection has the greatest potential to offer prolonged disease-free survival and thus an overall survival benefit across all stages.^{1–7} Surgical margins appear to be a highly significant factor in predicting survival.⁷ Positive margins, defined as the presence of tumor cells in the surrounding area following surgical resection, have been associated with increased local recurrence and decreased overall survival.^{2, 4, 6, 7} Therefore, negative surgical margins are considered to be of utmost importance in any cancer operation.

Differentiating normal tissue from tumor is the cornerstone of effective oncologic surgery and determining completeness of surgical resection. The recent interest in targeted tumor imaging techniques has resulted in new techniques that enable better identification of tumor lesions to improve diagnosis and treatment of pancreatic cancer from preoperative staging modalities^{8–11} to optimizing the surgeon's ability to visualize tumor margins at the initial operation.^{12–20}

In this proof-of-concept study, we inquired if fluorescence-guided surgery (FGS) could improve surgical outcomes and thus reduce recurrence rates in orthotopic mouse models of human pancreatic cancer expressing a genetic fluorescent reporter. A randomized active-control pre-clinical trial comparing bright light surgery (BLS) to FGS in an orthotopic mouse model of pancreatic cancer was utilized.

Methods

Cell Line and Cell culture—The BxPC-3 pancreatic cancer cell line was obtained from the American Type Culture Collection (Manassas, VA). Cells were maintained in DMEM media supplemented with 10% heat-inactivated fetal bovine serum and 1% penicillin and streptomycin (Life Technologies, Inc., Grand Island, NY). Cells were cultured at 37°C in a 5% CO₂ incubator.

RFP Retroviral Transduction and Selection of BxPC-3-RFP Pancreatic Cancer Cells—The pDsRed-2 vector (Clontech Laboratories, Inc., Palo Alto, CA) was used to engineer MIA-PaCa-2 clones stably expressing RFP. This vector expresses RFP and the neomycin resistance gene on the same bicistronic message and has been demonstrated to exhibit low toxicity in mammalian cell lines. pDsRed-2 was produced in PT67-packaging cells. RFP transduction was initiated by incubating 20% confluent BxPC-3 cells with retroviral supernatants of the packaging cells and DMEM for 24 h. Fresh medium was replenished at this time, and cells were allowed to grow in the absence of retrovirus for 12 h. This procedure was repeated until high levels of RFP expression, as determined using fluorescence microscopy, were achieved. Cells were then harvested by trypsin/EDTA and subcultured into selective 1828 medium that contained 200 µg/ml G418. The level of G418 was increased to 2000 µg/ml stepwise. Clones expressing high levels of RFP were isolated with cloning cylinders as needed and were amplified and transferred using conventional culture methods. High RFP-expression clones were isolated in the absence of G418 for 10 passages to select for stable expression of RFP *in vivo*.

Animal care

Female athymic *nu/nu* nude mice were maintained in a barrier facility on high-efficiency particulate air filtered racks. The animals were fed with autoclaved laboratory rodent diet (Teckland LM-485; Western Research Products, Orange, CA). All surgical procedures were performed under anesthesia with an intramuscular injection of 100 μ L of a mixture of 100 mg/kg ketamine and 10 mg/kg xylazine. For each procedure, 20 μ L of 1 mg/kg buprenorphine was administered for pain control. Euthanasia was achieved by 100% carbon dioxide inhalation, followed by cervical dislocation. All animal studies were conducted in accordance with the principles and procedures outlined in the National Institutes of Health (NIH) Guide for the Care and Use of Animals under assurance number A3873-01.

Orthotopic Tumor Implantation

Human BxPC-3-BxPC-3-RFP cancer cells were harvested by trypsinization and washed twice with serum-free medium. Viability was verified to be greater than 95% using the Vi-Cell XR automated cell viability analyzer (Beckman Coulter, Brea, CA). The cells were resuspended at 10^6 cells per 10 μ L of serum-free medium. Orthotopic human pancreatic cancer xenografts were established in nude mice by direct injection of fluorescent BxPC-3-RFP tumor cells into the pancreas. A small 6 to 10-mm transverse incision was made on the left flank of the mouse through the skin and peritoneum. The tail of the pancreas was exposed through this incision and 1×10^6 cells, mixed 1:1 with matrigel (BD Biosciences, Bradford MA) in a 10- μ L final volume, were injected into the pancreatic tail using a Hamilton syringe (Hamilton Co, Reno NV). Upon completion, the pancreas was returned to the abdomen and the incision was closed in two layers using 6.0 Ethibond non-absorbable sutures (Ethicon Inc., Somerville, NJ).

Tumor Resection

A total of 41 mice were used in the experiments; 20 of them underwent fluorescence-guided surgery (FGS) and the other 20 mice underwent bright light surgery (BLS). One mouse was sacrificed immediately after resection in order to be used to assess surgical margins by histology. Two weeks following orthotopic implantation of human pancreatic cancer cells, mice bearing BxPC-3 tumors were randomly assigned to the bright light surgery (BLS) group or to the fluorescence-guided surgery (FGS) group. Prior to resection of the pancreatic tumor, mice were anesthetized as described, and their abdomens were sterilized. The tail of the pancreas was delivered through a midline incision and the exposed pancreatic tumor was imaged preoperatively with the Olympus OV-100 Small Animal Imaging System (Olympus Corp, Tokyo Japan) under both standard bright field and fluorescence illumination. The investigators who evaluated the histology and the images were blinded to treatment assignments. Resection of the primary pancreatic tumor was performed using the MVX-10 fluorescence-dissecting microscope (Olympus) under bright light illumination for the BLS group and under fluorescence illumination through an RFP filter (excitation HQ 545/30x; emission 620/60m) for the FGS group. Postoperatively, the surgical resection bed was imaged with the OV-100 Small Animal Imaging System under both standard bright field and fluorescence illumination to assess completeness of surgical resection.

Postoperative Chemotherapy Treatment

Half of the BLS and FGS mice (ten mice in each group) were randomly selected to undergo four weeks of adjuvant chemotherapy using gemcitabine (Figure 1). Gemcitabine (Gemzar, Eli Lilly) was reconstituted in PBS at a concentration of 30 μ g/ μ L. Starting on postoperative day 1, mice received 150 mg/kg of gemcitabine twice weekly for four weeks via intraperitoneal injections. This dosing regimen was previously shown to have significant

activity against RFP-expressing pancreatic tumorgrafts without causing significant toxicity in the mice.²¹

Animal Imaging

To assess for recurrence and to follow tumor progression postoperatively, weekly whole body imaging of the mice was obtained with the Olympus OV-100 Small Animal Imaging System (Olympus Corp, Tokyo Japan), containing an MT-20 light source (Olympus Biosystems, Planegg Germany) and DP70 CCD camera (Olympus Corp.). Seven weeks after resection and after completion of the four-week gemcitabine treatment regimen, the mice were sacrificed and intravital images were taken to evaluate primary pancreatic and metastatic tumor burden. All images were analyzed with Image J v1.440 (National Institutes of Health, Bethesda, MD).

Tissue histology

For histologic examination of surgical margins, tumor samples were surgically removed en bloc with surrounding tissue at the time of resection in an additional mouse that was not included in the randomization of the 40 mice. The surgeon exposed the surgical field but remained in a separate area during the pre-surgical imaging. OV100 imaging of the surgical area was performed prior to resection and the mouse was then returned to the surgeon. Following resection, both the surgical field and the resected specimens were again imaged on the OV100 using brightfield and fluorescence light settings. The mouse was then terminated, the surgical margins inked, and the tissues processed for permanent sectioning. Fresh tissue samples were fixed in Bouins solution and regions of interest embedded in paraffin prior to sectioning and staining with H&E for standard light microscopy. H&E-stained permanent sections were examined using an Olympus BX41 microscope equipped with a Micropublisher 3.3 RTV camera (QImaging, Surrey, B.C., Canada). All images were acquired using QCapture software (QImaging) without post-acquisition processing. The investigators who evaluated the histology and the images were blinded to treatment assignment.

Data processing & statistical analysis

PASWStatistics 18.0 (SPSS, Inc.) or R v. 2.11.0 were used for statistical analyses. Tumor burden is expressed as either median (range) or mean \pm SEM. A Welch's t-test was used to compare continuous variables between two groups; ANOVA models were used to compare multiple groups. Comparisons between categorical variables were analyzed using Fisher's exact test. Survival outcomes were compared using log rank tests with confidence intervals computed by the method of Brookmeyer and Crowley²² using the surv function in R. Hazard ratios with their 95% confidence intervals were estimated using Cox proportional hazards models. A p-value of ≤ 0.05 was considered statistically significant for all comparisons.

Results

Primary Tumor Resection

The first aim of the present study was to evaluate the effectiveness of fluorescence-guided surgery (FGS) for complete surgical resection of pancreatic cancer in the orthotopic mouse models. To achieve this goal, orthotopic mouse models of human pancreatic cancer using brightly red-fluorescent BxPC-3 pancreatic cancer cells were established in 40 mice (Figure 1). Two weeks post implantation of 1×10^6 cancer cells, the mice were randomly selected to undergo bright light surgery (BLS) or FGS (20 mice in each group). There was no significant difference in preoperative tumor burden among the surgical groups ($p=0.705$).

The mean tumor burden for the FGS group was $11.7 \pm 1.0 \text{ mm}^2$ versus $10.7 \pm 2.4 \text{ mm}^2$ for the BLS group (Figure 2a).

Significant improvement in visualization of primary pancreatic tumor lesions, allowing enhanced distinction of tumor from surrounding normal pancreatic tissue, was achieved in the FGS group (Figure 2b). The significantly-enhanced localization during FGS permitted a more complete resection of tumor resulting in a significant difference in postoperative tumor burden among the surgical groups. A mean postoperative tumor burden of $0.1 \pm 0.06 \text{ mm}^2$ was achieved in the FGS group. In contrast, tumor reduction in the BLS group was not as successful, achieving a mean postoperative tumor burden of $2.6 \pm 0.6 \text{ mm}^2$ ($p=0.001$) (Figure 2a).

Over 98% of pancreatic cancer was removed under FGS compared to only 77% under BLS ($p=0.005$). As seen in Figure 2b, the mouse received a complete resection (F0) using FGS without experiencing a large removal of normal pancreatic tissue.

To further evaluate the completeness surgical resection under FGS, mice were categorized by the extent of the remaining tumor burden on postoperative images analyzed by ImageJ. An F0 resection was defined as a complete absence of tumor in the postsurgical bed as detected by fluorescence imaging at 14x magnification using the OV-100. Postoperative tumor burden $>0 \text{ mm}^2$ but less than 1 mm^2 was defined as an F1 resection. We determined this category to be equivalent to microscopic disease. Gross disease (tumor burden value $>1 \text{ mm}^2$) was categorized as an F2 resection (Figure 3).

Under BLS, no F0 resections were achieved. Furthermore, in the BLS group, more mice (63%) had evidence of gross disease (F2 resection) post resection than in FGS group, and the remaining 37% were left with minimal residual disease (F1 resection). In the FGS group, 20% of the mice had an F0 resection, 75% had an F1 resection and 5% (1 mouse) had evidence of gross disease left behind (Table 1). Overall, there was a significant association of improved surgical resection with FGS compared to BLS ($p=0.001$).

Disease at Termination

FGS resulted in a decreased mean tumor burden in the pancreas at termination compared to BLS. The mean tumor burden in the pancreas at termination (7 weeks postoperatively) in the BLS group was $19.3 \pm 5.3 \text{ mm}^2$ versus $6.2 \pm 3.6 \text{ mm}^2$ in the FGS group ($p=0.048$) (Figure 4). The surgeon's enhanced ability to remove tumor from the pancreas also resulted in a significantly longer disease-free survival in mice from the FGS group compared to mice from the BLS group ($p=0.02$, hazard ratio=0.39, 95% CI: [0.17, 0.88]). The median disease-free survival in mice from the BLS group was 1 week (95% CI: [1 week, ∞]), while disease-free survival of the mice in the FGS was 7 weeks (95% CI: [3 weeks, ∞]), (Figure 5).

Adjuvant gemcitabine did not improve outcomes of animals with incomplete resections in either the FGS or BLS groups.

In order to correlate imaging results with tissue histology, a mock experiment was performed in which the mice were terminated immediately following surgical resection of tumors. This allowed for a comparison of imaging results with histology for assessing the completeness of either bright light or fluorescence-guided surgical tumor resection. Figures 6a and 6b show the brightfield (lower triptych) and fluorescence (upper triptych) images obtained at the time of surgery for either a bright light or fluorescence-guided surgical approach, respectively. The separate histology images shown in both 6a and 6b are histologic cross-sections taken through the surgical margins of the unresected tissues, tissues

which would have remained in the mouse had this been a survival surgery experiment. For the BLS experiment shown in Figure 6a, post-resection imaging showed focal fluorescent residual disease indicating unresected tumor. A tissue cross-section of the fluorescent area was used for histology. Histology confirmed the presence of a nodule of abnormal tissue present at the site of the fluorescent signal seen during post-resection imaging. In contrast, fluorescence imaging and the corresponding histologic sections (Figure 6b) did not show any residual tumor after FLS.

Discussion

Despite the extensive research to develop improved systemic therapies of pancreatic cancer, surgical resection remains the only treatment offering a survival advantage (5-year survival range, 15–25%) and chances for cure.²³ The cornerstone of oncologic surgery is complete resection of tumor. Surgical margins can drastically alter the patient's postoperative survival. Negative surgical margins have been noted by many to be strongly associated with a survival advantage in patients suffering from pancreatic adenocarcinoma.²⁴

Benassai and colleagues²⁵ followed 75 of their patients after pancreaticoduodenectomy for pancreatic head carcinoma and reported an overall median survival of 17 months and a 5-year survival of 18.7%. Patients with negative margins had an increase in median survival to 26 months and an actuarial 5-year survival of 23.3% (n=60) whereas no patient with positive margins (n=15) survived at 13 months. Multivariate analysis indicated that the presence of positive resection margins was the strongest independent predictor of decreased survival (hazard ratio = 2.29, p=0.0002). Chen, et al.²⁶ performed sequential margin analysis and revealed that the long-term survival difference became significant when the margin was clear by 2 mm (p<0.01) while at a margin of <1 mm there was no statistical difference in long-term survival. Furthermore, Sperti and colleagues²⁷ analyzed the pattern of failure and the clinicopathologic factors that influenced disease-free survival in 78 patients who died after macroscopic curative resection for pancreatic cancer. They confirmed with multivariate analysis that radicality of resection was an independent and significant predictor of disease-free survival (p=0.04). Other authors have also suggested the importance of complete surgical resection in predicting survival outcomes.^{28–31}

In an effort to improve the intraoperative detection of surgical margins, researchers have studied the use of fluorescent probes that can be administered in situ and make tumors selectively fluorescent.²⁰ A variety of labeling compounds have been used for fluorescence-guided surgery in human subjects. For example, sentinel lymph nodes in breast cancer patients were detected and labeled by the near-infrared fluorescing dye indocyanine as well as by 99mTC-lymphoscintigraphy.³² However, indocyanine does not specifically label tumor cells. In contrast, the metabolite 5-aminolevulinic acid, a precursor of hemoglobin, results in accumulation of porphyrins within malignant glioma. Porphyrin fluorescence in glioma can then be visualized by use of a modified neurosurgical microscope. In one study, glioma patients were given 5-aminolevulinic acid orally 3 h before induction of anaesthesia.³³ Patients undergoing fluorescence-guided surgery had their tumor resected completely in 65% of 139 cases compared with 36% of 131 who underwent bright light surgery. Patients who underwent fluorescence-guided surgery had higher, 6-month progression-free survival (41%) than did those who had surgery under white light (21%).³³

Other more tumor-specific approaches to fluorescence-guided surgery have been described as well. Activatable cell-penetrating peptides (ACPPs) were used to label breast tumors in a mouse model. The labeled tumors could be resected under fluorescence guidance which resulted in better long-term tumor-free survival and overall survival than animals whose tumors were resected with brightfield illumination only.¹⁵

Our group described the use of a monoclonal antibody specific for either CA19-9 or CEA conjugated to a green fluorophore and delivered i.v. to nude mice with orthotopic human pancreatic or colon tumors.^{12, 14} Fluorescent tumors, which were invisible using standard brightfield imaging, demonstrated clear fluorescence. The labeled tumors were resected under fluorescence guidance.¹² In another study, fluorophore-conjugated anti-CEA antibodies improved accuracy of laparoscopic staging in a mouse model of pancreatic cancer.¹⁸

Genetic labeling of tumors with green fluorescent protein (GFP) in situ has also been achieved. Stiles et al³⁴ used a herpes simplex virus (NV1066), carrying the *gfp* gene to label metastatic lung tumor foci of less than one mm in a mouse model. The labeled tumors were detected by using a thoracoscopic endoscope system equipped with fluorescent filters. Kishimoto et al., selectively and accurately labeled tumors with GFP, using a telomerase-dependent adenovirus (OBP-401) containing the *gfp* gene.¹³ The labeled tumors could then be resected under fluorescence guidance. Kishimoto et al also demonstrated that tumors which recurred after fluorescence-guided surgery maintained GFP expression.³⁵ Therefore, the detection of recurrence and future metastasis is also possible with OBP-401 GFP labeling, since recurrent cancer cells stably express GFP. Maintenance of label in recurrent tumors is not possible with non-genetic probes.

The study is novel as it is the first study to look at FGS in a mouse model of pancreatic cancer. The study is also novel with regard to the significant results observed with the extent that FGS increased survival.

The techniques described in this manuscript have clinical applicability to pancreatic cancer. For instance, we envision that FGS would be helpful in assessing the need for vascular resection in pancreatic cancer. The ideal fluorescent probe would need to be sensitive enough to distinguish between fibrosis from pancreatitis and infiltrative tumor along major vascular structures. FGS could be used for diagnostic purposes to help in the difficult cases in which there is no preoperative diagnosis of cancer, and the differential diagnosis includes chronic pancreatitis vs. cancer. Further studies are necessary to determine if this technology has the ability to assess the extent of IPMN, or does it require tumor nodules of a certain minimum size. A potential solution to the above problems is the use of a tumor-specific telomerase-dependent adenovirus we have developed that selectively labels on cancer cells with green fluorescent protein (GFP).^{13, 20} Lastly, FGS could be used to assure that all involved regional nodes within the resection field are appropriately extirpated.

Conclusions

The present study demonstrated that fluorescence-guided surgery improved surgical outcomes and reduced recurrence rates and extended disease-free survival in orthotopic mouse models of human pancreatic cancer. A significant decrease in postoperative tumor burden ($p=0.001$) and pancreatic tumor burden at termination ($p=0.048$) was achieved in the FGS groups compared to the BLS groups. Fluorescence guided surgery allowed us to identify and remove sub-millimeter size tumor deposits throughout the pancreas. This study demonstrated that by enhancing the surgeon's ability to distinguish normal pancreatic tissue from tumor led to a more complete tumor resection and thus subsequent improved disease-free survival and decreased tumor burden at termination. This novel approach has significant potential to improve outcomes in the surgical treatment of clinical cancer. Our future goals are to utilize unique characteristics of pancreatic cancer, such as telomerase expression which enables selective expression of a GFP-containing adenovirus^{13, 35, 36} or expression of CEA or CA 19-9 antigens which can bind fluorophore-conjugated antibodies^{12, 14, 18}, to

fluorescently label the tumor in order to more effectively delineate surgical margins for improved long-term outcomes.

Acknowledgments

Work supported in part by grants from the National Cancer Institute CA142669 and CA132971 (to Dr Bouvet and AntiCancer, Inc) and T32 training grant CA121938-5 (to Dr Metildi).

References

1. Sener SF, Fremgen A, Menck HR, Winchester DP. Pancreatic cancer: a report of treatment and survival trends for 100,313 patients diagnosed from 1985–1995, using the National Cancer Database. *J Am Coll Surg.* 1999; 189:1–7. [PubMed: 10401733]
2. Adham M, Jaeck D, Le Borgne J, et al. Long-term survival (5–20 years) after pancreatectomy for pancreatic ductal adenocarcinoma: a series of 30 patients collected from 3 institutions. *Pancreas.* 2008; 37:352–357. [PubMed: 18665012]
3. Cartwright T, Richards DA, Boehm KA. Cancer of the pancreas: are we making progress? A review of studies in the US Oncology Research Network. *Cancer Control.* 2008; 15:308–313. [PubMed: 18813198]
4. Conlon KC, Klimstra DS, Brennan MF. Long-term survival after curative resection for pancreatic ductal adenocarcinoma. Clinicopathologic analysis of 5-year survivors. *Ann Surg.* 1996; 223:273–279. [PubMed: 8604907]
5. Di Marco M, Di Cicilia R, Macchini M, et al. Metastatic pancreatic cancer: is gemcitabine still the best standard treatment? (Review). *Oncol Rep.* 2010; 23:1183–1192. [PubMed: 20372829]
6. Shimada K, Sakamoto Y, Nara S, et al. Analysis of 5-year survivors after a macroscopic curative pancreatectomy for invasive ductal adenocarcinoma. *World J Surg.* 2010; 34:1908–1915. [PubMed: 20376443]
7. Yeo CJ, Cameron JL, Lillemoe KD, et al. Pancreaticoduodenectomy for cancer of the head of the pancreas. 201 patients. *Ann Surg.* 1995; 221:721–731. discussion 731–733. [PubMed: 7794076]
8. Jiang T, Olson ES, Nguyen QT, et al. Tumor imaging by means of proteolytic activation of cell-penetrating peptides. *Proc Natl Acad Sci U S A.* 2004; 101:17867–17872. [PubMed: 15601762]
9. Kennedy MD, Jallad KN, Thompson DH, et al. Optical imaging of metastatic tumors using a folate-targeted fluorescent probe. *J Biomed Opt.* 2003; 8:636–641. [PubMed: 14563201]
10. Kishimoto H, Kojima T, Watanabe Y, et al. In vivo imaging of lymph node metastasis with telomerase-specific replication-selective adenovirus. *Nat Med.* 2006; 12:1213–1219. [PubMed: 17013385]
11. Olson ES, Aguilera TA, Jiang T, et al. In vivo characterization of activatable cell penetrating peptides for targeting protease activity in cancer. *Integr Biol (Camb).* 2009; 1:382–393. [PubMed: 20023745]
12. Kaushal S, McElroy MK, Luiken GA, et al. Fluorophore-conjugated anti-CEA antibody for the intraoperative imaging of pancreatic and colorectal cancer. *J Gastrointest Surg.* 2008; 12:1938–1950. [PubMed: 18665430]
13. Kishimoto H, Zhao M, Hayashi K, et al. In vivo internal tumor illumination by telomerase-dependent adenoviral GFP for precise surgical navigation. *Proc Natl Acad Sci U S A.* 2009; 106:14514–14517. [PubMed: 19706537]
14. McElroy M, Kaushal S, Luiken GA, et al. Imaging of primary and metastatic pancreatic cancer using a fluorophore-conjugated anti-CA19-9 antibody for surgical navigation. *World J Surg.* 2008; 32:1057–1066. [PubMed: 18264829]
15. Nguyen QT, Olson ES, Aguilera TA, et al. Surgery with molecular fluorescence imaging using activatable cell-penetrating peptides decreases residual cancer and improves survival. *Proc Natl Acad Sci U S A.* 2010; 107:4317–4322. [PubMed: 20160097]
16. Tran Cao HS, Kaushal S, Lee C, et al. Fluorescence laparoscopy imaging of pancreatic tumor progression in an orthotopic mouse model. *Surg Endosc.* 2011; 25:48–54. [PubMed: 20533064]

17. Tran Cao HS, Kaushal S, Menen RS, et al. Submillimeter-resolution fluorescence laparoscopy of pancreatic cancer in a carcinomatosis mouse model visualizes metastases not seen with standard laparoscopy. *J Laparoendosc Adv Surg Tech A*. 2011; 21:485–489. [PubMed: 21699431]
18. Tran Cao HS, Kaushal S, Metildi CA, et al. Fluorophore-conjugated anti-CEA antibody improves accuracy of staging laparoscopy in a mouse model of pancreatic cancer. *Ann Surg Oncol*. 2011; 18:S40.
19. van Dam GM, Themelis G, Crane LM, et al. Intraoperative tumor-specific fluorescence imaging in ovarian cancer by folate receptor-alpha targeting: first in-human results. *Nat Med*. 2011; 17:1315–1319. [PubMed: 21926976]
20. Bouvet M, Hoffman RM. Glowing tumors make for better detection and resection. *Sci Transl Med*. 2011; 3:110fs10.
21. Katz MH, Takimoto S, Spivack D, et al. A novel red fluorescent protein orthotopic pancreatic cancer model for the preclinical evaluation of chemotherapeutics. *J Surg Res*. 2003; 113:151–160. [PubMed: 12943825]
22. Brookmeyer R, Crowley J. A confidence interval for the median survival time. *Biometrics*. 1982; 38:29–41.
23. Loos M, Kleeff J, Friess H, Buchler MW. Surgical treatment of pancreatic cancer. *Ann N Y Acad Sci*. 2008; 1138:169–180. [PubMed: 18837898]
24. Garcea G, Dennison AR, Pattenden CJ, et al. Survival following curative resection for pancreatic ductal adenocarcinoma. A systematic review of the literature. *Jop*. 2008; 9:99–132. [PubMed: 18326920]
25. Benassai G, Mastrorilli M, Quarto G, et al. Factors influencing survival after resection for ductal adenocarcinoma of the head of the pancreas. *J Surg Oncol*. 2000; 73:212–218. [PubMed: 10797334]
26. Chen JW, Bhandari M, Astill DS, et al. Predicting patient survival after pancreaticoduodenectomy for malignancy: histopathological criteria based on perineural infiltration and lymphovascular invasion. *HPB (Oxford)*. 2010; 12:101–108. [PubMed: 20495653]
27. Sperti C, Pasquali C, Piccoli A, Pedrazzoli S. Recurrence after resection for ductal adenocarcinoma of the pancreas. *World J Surg*. 1997; 21:195–200. [PubMed: 8995078]
28. Jamieson NB, Foulis AK, Oien KA, et al. Positive mobilization margins alone do not influence survival following pancreaticoduodenectomy for pancreatic ductal adenocarcinoma. *Ann Surg*. 2010; 251:1003–1010. [PubMed: 20485150]
29. Mannell A, van Heerden JA, Weiland LH, Ilstrup DM. Factors influencing survival after resection for ductal adenocarcinoma of the pancreas. *Ann Surg*. 1986; 203:403–407. [PubMed: 3008674]
30. Matsuno S, Sato T. Surgical treatment for carcinoma of the pancreas. Experience in 272 patients. *Am J Surg*. 1986; 152:499–504. [PubMed: 2430481]
31. Sommerville CA, Limongelli P, Pai M, et al. Survival analysis after pancreatic resection for ampullary and pancreatic head carcinoma: an analysis of clinicopathological factors. *J Surg Oncol*. 2009; 100:651–656. [PubMed: 19722229]
32. Troyan SL, Kianzad V, Gibbs-Strauss SL, et al. The FLARE intraoperative near-infrared fluorescence imaging system: a first-in-human clinical trial in breast cancer sentinel lymph node mapping. *Ann Surg Oncol*. 2009; 16:2943–2952. [PubMed: 19582506]
33. Stummer W, Pichlmeier U, Meinel T, et al. Fluorescence-guided surgery with 5-aminolevulinic acid for resection of malignant glioma: a randomised controlled multicentre phase III trial. *Lancet Oncol*. 2006; 7:392–401. [PubMed: 16648043]
34. Stiles BM, Adusumilli PS, Bhargava A, et al. Minimally invasive localization of oncolytic herpes simplex viral therapy of metastatic pleural cancer. *Cancer Gene Ther*. 2006; 13:53–64. [PubMed: 16037824]
35. Kishimoto H, Aki R, Urata Y, et al. Tumor-selective, adenoviral-mediated GFP genetic labeling of human cancer in the live mouse reports future recurrence after resection. *Cell Cycle*. 2011; 10:2737–2741. [PubMed: 21785265]
36. Kishimoto H, Urata Y, Tanaka N, et al. Selective metastatic tumor labeling with green fluorescent protein and killing by systemic administration of telomerase-dependent adenoviruses. *Mol Cancer Ther*. 2009; 8:3001–3008. [PubMed: 19887549]

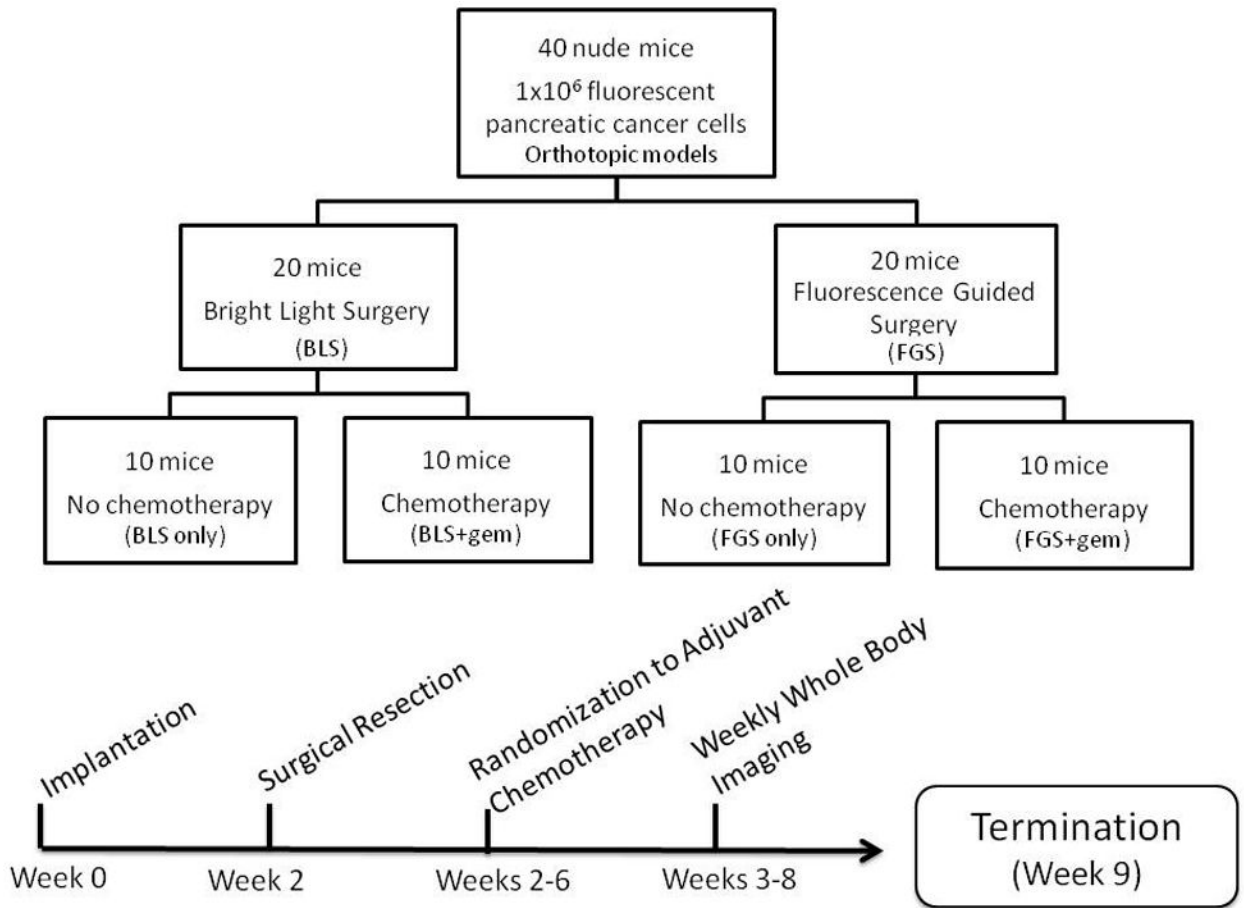


Figure 1.

Schematic diagram of study timeline. Two weeks post orthotopic tumor implantation, the mice were randomized and tumors were resected using the MVX 10 dissecting microscope. Starting on POD 1, half of the mice from each surgical arm underwent 4 weeks of gemcitabine treatment. At week 9 (or 7 weeks postoperatively) the mice were sacrificed for intravital imaging to evaluate extent of tumor burden in the pancreas. During the entire postoperative period, all mice were imaged weekly using the OV-100.

Figure 2a

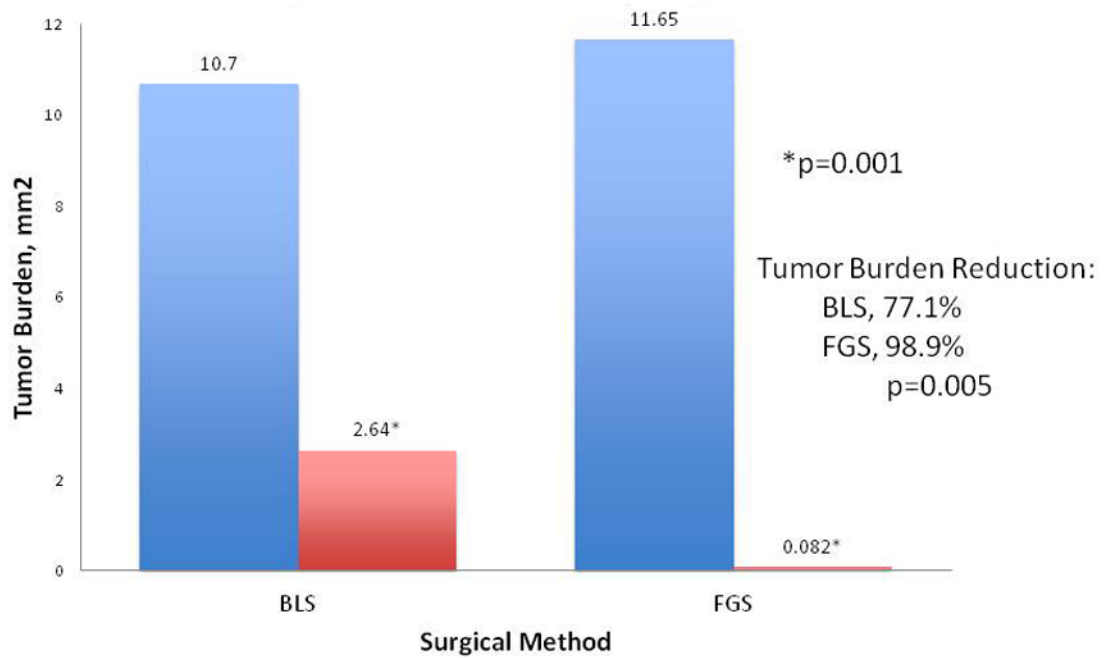
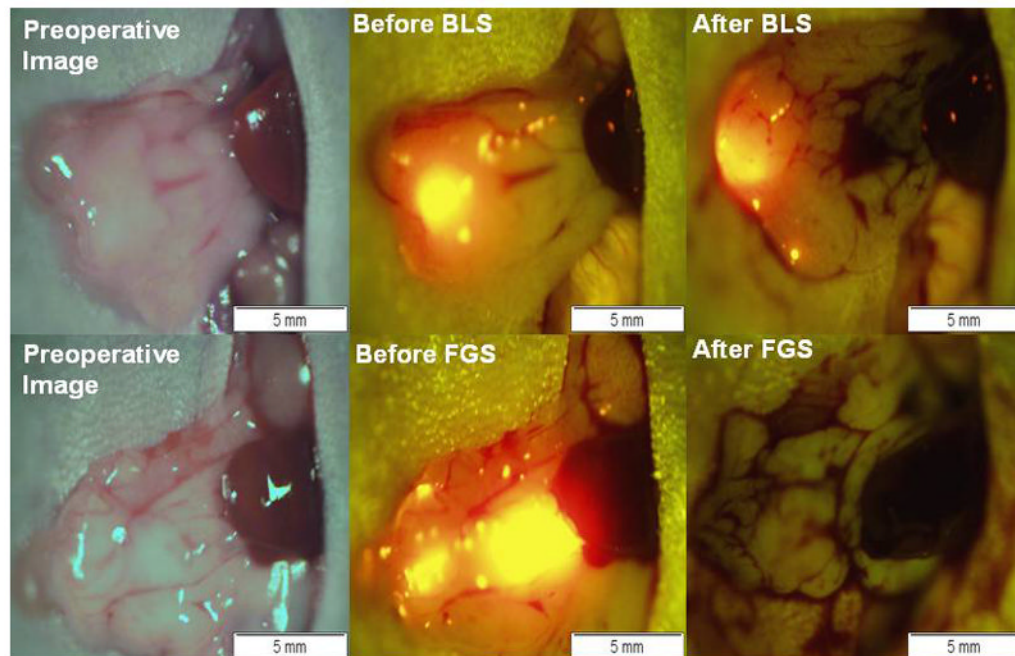


Figure 2b

**Figure 2.**

(A) Pre- and postoperative tumor burden by surgical method. The mean postoperative tumor burden under BLS was $2.6 \pm 0.6 \text{ mm}^2$, a significantly higher value than the mean postoperative tumor burden achieved under FGS ($0.08 \pm 0.06 \text{ mm}^2$). Asterisk indicates statistical significance with $p=0.001$. On average, 77% of the tumor burden was resected

under BLS. More than 98% tumor burden reduction was achieved with FGS ($p=0.005$). (B) Preoperative and postoperative images of the pancreas in two different mouse specimens under different surgical methods. The top row contains representative pre- and postoperative images of a specimen from the BLS group. A tumor reduction of only 77% was achieved in the BLS group. The bottom row images are representative pre- and postoperative images of a specimen from the FGS group. A significant improvement in tumor reduction was achieved in this group (98.9%, $p=0.005$). A complete surgical resection of pancreatic tumor with negative surgical margins was achieved in this mouse without requiring significant resection of the pancreas. All images were analyzed for tumor burden using ImageJ. Blue bar, preoperative tumor burden; red bar, postoperative tumor burden.

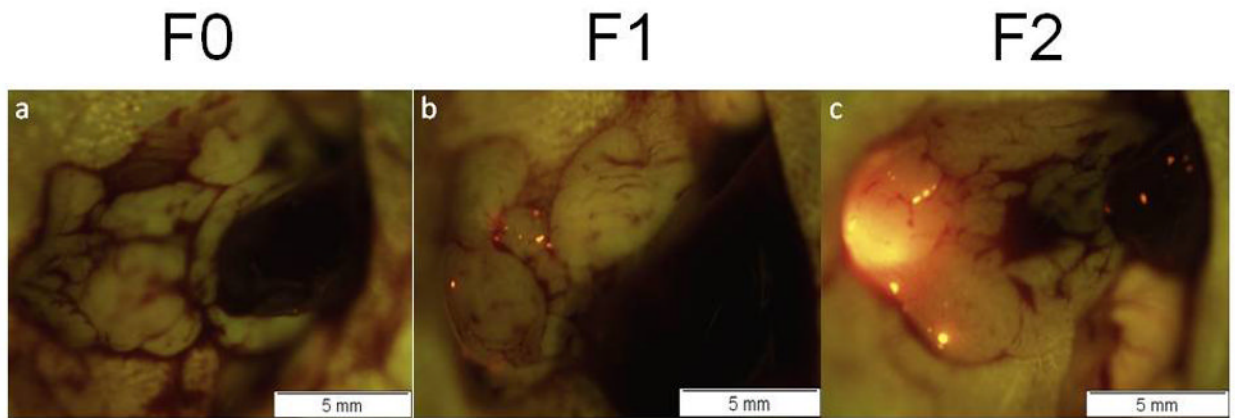


Figure 3.

Representative OV-100 images of resection outcomes categorized by the remaining disease analyzed by ImageJ from postoperative images. (a) F0 resection was defined as a complete absence of fluorescent tumor in the postsurgical bed. (b) F1 resection was defined as postoperative tumor burden $>0 \text{ mm}^2$ but less than 1 mm^2 . The specimen in this image had a postoperative tumor burden of 0.110 mm^2 . (c) F2 resection was defined as postoperative tumor burden $>1 \text{ mm}^2$. The mouse specimen in this image had a postoperative tumor burden of 2.778 mm^2 .

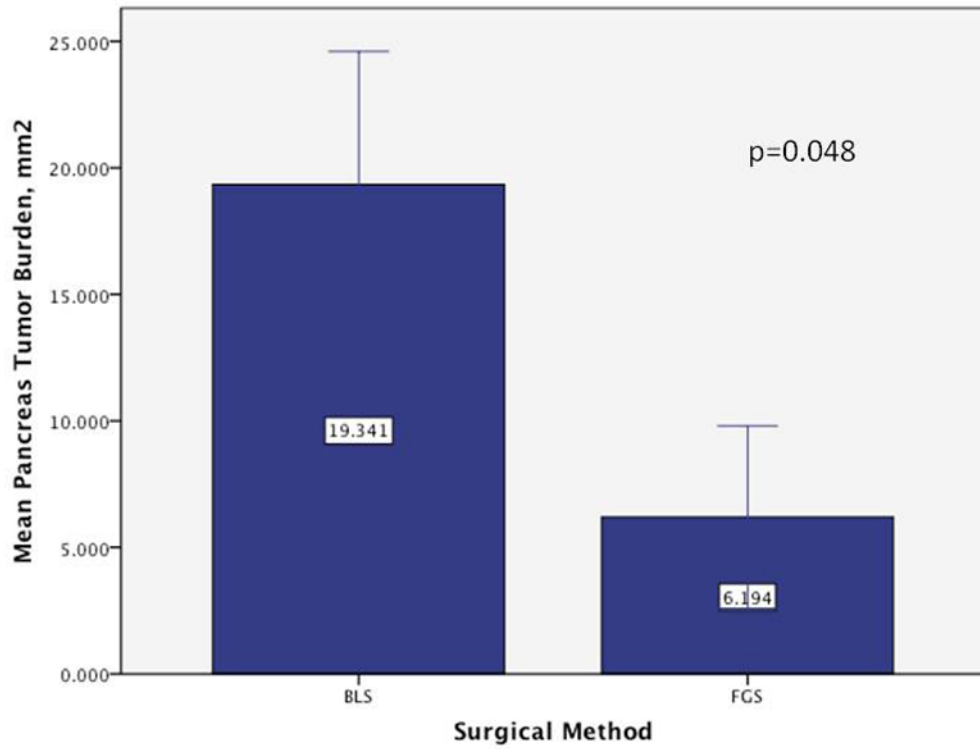


Figure 4.

Extent of tumor burden by surgical method in the pancreas at time of termination. The BLS group had significantly greater tumor burden in the pancreas at termination compared to the FGS group ($p=0.048$). The improved resection under FGS at the initial operation had a significant effect on recurrence, disease-free survival and overall extent of disease in the pancreas. Error bars: ± 1 SE.

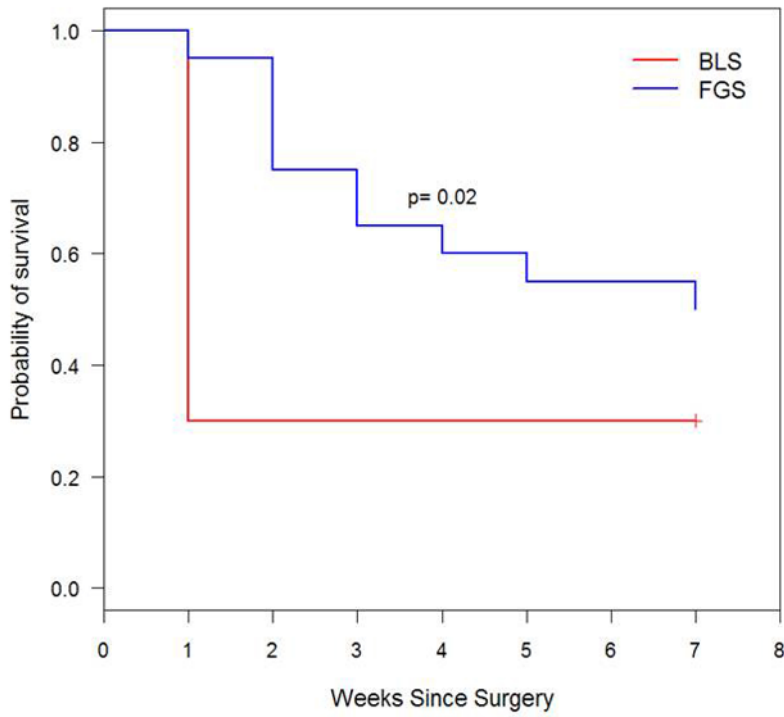


Figure 5. Kaplan-Meier disease-free survival curve. FGS lengthened disease-free survival from 1 week (95% CI, 1 week) to 7 weeks (95% CI, 3 weeks). By termination date, 70% of the mice in the BLS group had evidence of tumor recurrence based on images obtained with the OV-100 Small Animal Imaging System, while 50% had recurred in the FGS group.

Figure 6a

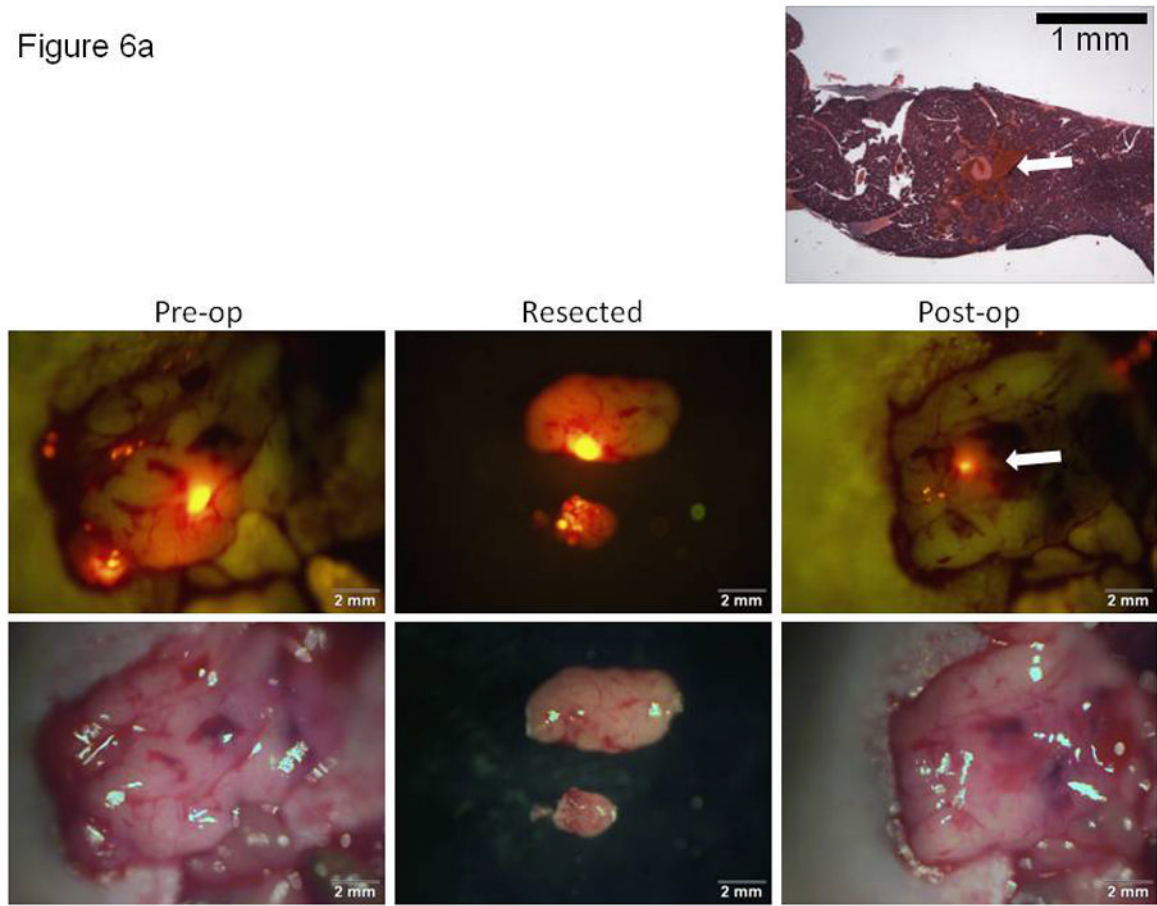
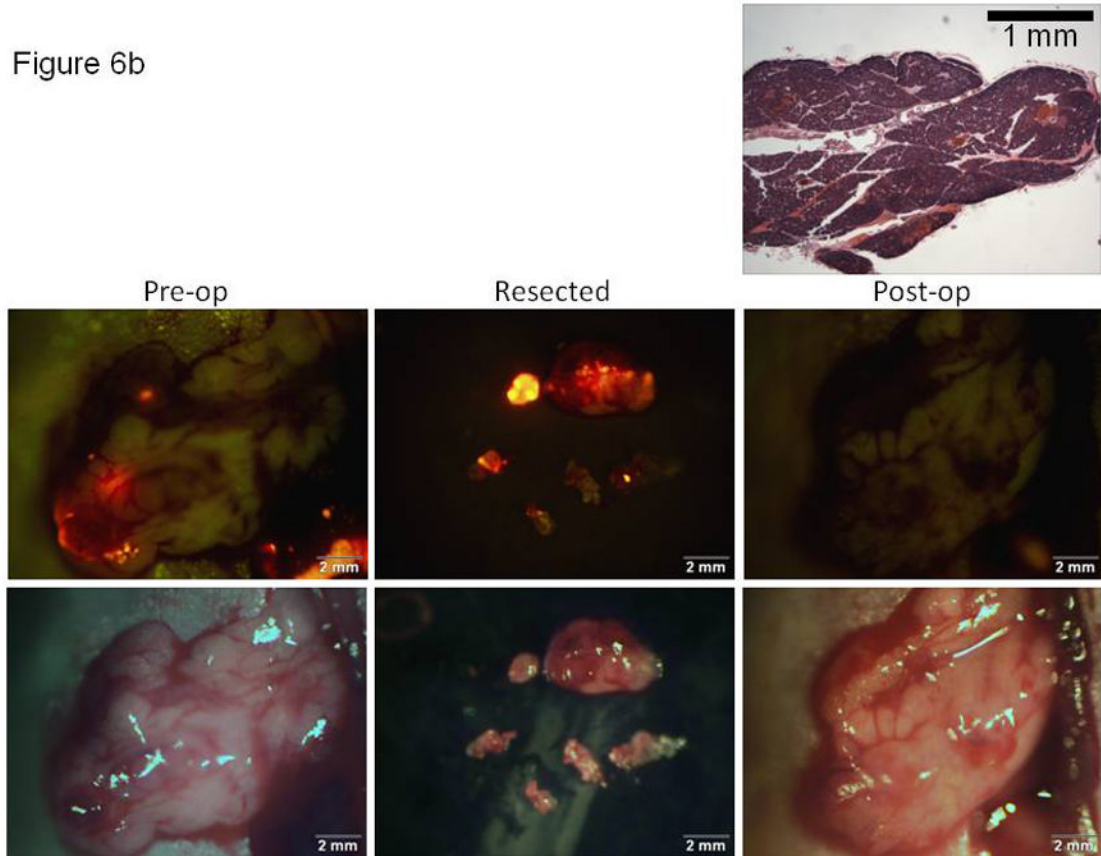


Figure 6b

**Figure 6.**

Correlation of imaging with histology for documentation of tumor resection using either bright light or fluorescence-guided surgical techniques. Brightfield (lower) and fluorescence (upper) images obtained at the time of surgery for either (A) a bright light or (B) fluorescence-guided surgical approach. Histologic cross-sections (top image in each 6A and 6B, H&E) taken through the surgical margins of the unresected tissues. The arrows in Figure 6A show the correlation of the small focus of unresected (fluorescent) tumor cells retained in the post-operative tumor bed and the histologic section through this focus in a mouse resected for tumor under BLS.

Table 1

Resection Type Achieved by Surgical Method

Surgical Method	F0 Resection	F1 Resection	F2 Resection
Bright light surgery	0	7 (36.8%)	12 (63.2%)
Fluorescence guided surgery	4 (20%)	15 (75%)	1 (5%)

* An F0 resection was defined as a complete absence of tumor in the postsurgical bed as detected by fluorescence at 14x magnification using the OV-100 image and image J software. A postoperative tumor burden $>0 \text{ mm}^2$ but less than 1 mm^2 was defined as an F1 resection (microscopic disease). Gross disease (tumor burden $>1 \text{ mm}^2$) was categorized as an F2 resection.